

## Vacuum switch performance in a 1.2 MJ pulse forming network

David W. Scholfield,<sup>1</sup> Michael D. Butcher,<sup>1</sup> Brian Hilko,<sup>2</sup> and Greg Dorr<sup>1</sup>

<sup>1</sup>Science Applications International Corporation, 2445 Alamo Ave. SE, Albuquerque, New Mexico 87106, USA

<sup>2</sup>Science Applications International Corporation, Suite N, 12000 Indian Creek Court, Beltsville, Maryland 20705, USA

(Received 18 September 2007; accepted 14 January 2008; published online 29 February 2008)

Vacuum switching has been used since the early days of pulsed power to provide a means to controlling the flow of large amounts of current. The attractions of vacuum switches for high energy switching are the vacuum mitigates mechanical shock generated by the discharge, low erosion rates, and rapid recovery for repetitive rate operations. Some of the drawbacks of vacuum switching are typically the requirement of a vacuum system and metal vapor sputtering which eventually renders the switch unusable. SAIC has developed a compact vacuum switch which is capable of conducting a current pulse in excess of 300 kA peak for a duration of approximately 0.5 ms. On a single shot, 150 C have been switched while the amount of action seen by these switches has been as much as  $3.65 \times 10^7 \text{ A}^2 \text{ s}$ . Switches of this design have been able to conduct up to 20 pulses of this magnitude before failure has occurred. The switch is triggerable down to 80 V potential across the anode and cathode. This paper describes the development of this switch. © 2008 American Institute of Physics. [DOI: 10.1063/1.2839916]

### INTRODUCTION

There are many switching techniques available for use in pulsed power applications. Among these are spark gap switching, solid and liquid dielectric switching, solid state switching, and vacuum switching. Vacuum switching occurs when the mean free path of a molecule of insulating gas is greater than that of the interelectrode gap.<sup>1</sup> This regime has been popularly represented as that region of the Paschen curve to the left of the Paschen minimum, as illustrated in Fig. 1. Vacuum switch design appears to have begun to stagnate in recent times due to the near term development of solid state switches,<sup>2-7</sup> which are rapidly achieving ever greater voltage hold off and current carrying capabilities. Despite progress within the solid state switch community, there is still a demand for high current operations that cannot yet be met by this technology. SAIC's needs required switches which were capable of switching 1.2 MJ of energy onto a bus with high reliability and repeatability, and yet were able to meet stringent weight and volume requirements. Of the options available<sup>8-14</sup> none appeared to be capable of meeting all the requirements.

The switch designed for this effort was originally required to withstand a peak voltage of 20 kV, carry 95 kA peak current with an action of  $2.7 \times 10^6 \text{ A}^2 \text{ s}$ . The overall pulse length was specified to be 0.5 ms. Vacuum switching was the technology selected as the solid state switch candidates required additional time to mature, and the pressures required by gas switching to achieve the desired performance were deemed to be too high for the levels of energy to be utilized. This necessitated a development effort to produce a vacuum switch which could satisfy not only the electrical requirements of the program but also the imposed mechanical constraints.

### DISCUSSION

The pulse forming network employed for this project was a type E pulse forming network (PFN) that utilized capacitors of 500  $\mu\text{F}$  and inductors of 400 nH. The charge voltage across each capacitor was 16 kV. The PFN would contain three switches. The probability of a system failure due to a malfunction of a vacuum switch was required to be less than 1%. Thus, the probability of an individual switch malfunctioning could only be allowed to be 0.013%. Each switch may malfunction only 13 times in approximately every 100 000 discharges, a difficult goal to achieve for vacuum switches in the pulsed power environment. To satisfy the requirements for reliable operation several design features were incorporated into the switch.

Assembly drawings of the switch are illustrated in Figs. 2 and 3. In Fig. 2 the anode is shown on the left, with the insulator residing in the middle, and the cathode on the right. Figure 3 illustrates an assembled switch with an external clamping mechanism constructed of two nylon 6 rings. The

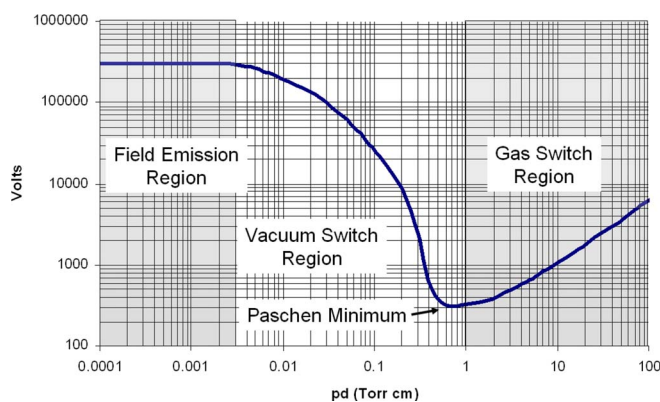


FIG. 1. (Color online) Paschen curve for air.

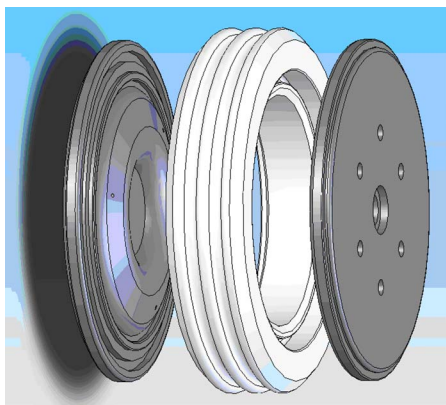


FIG. 2. (Color online) Electrode and insulator arrangement.

electrodes and insulator are sandwiched in between the clamp with the anode at the top of the figure. 12 bolts along the outer diameter of the nylon 6 rings held the assembly in place. The overall dimensions of the assembled switch are 14.27 cm in diameter, 4.77 cm thick, with an interelectrode of 1.59 cm.

A common failure mode of vacuum switches is surface tracking from electrode to electrode across a contaminated insulator, the contamination occurring due to deposition of electrode material as a consequence of the discharges. Many techniques have been used in the past to provide protection for the insulator from this deposition.<sup>12,15</sup> Building upon this research the current design incorporated a blast shield to ensure that the risk of a short from electrode to electrode across the insulator was minimized. The addition of the blast ring on the inside radius of the insulator provided for the interception of any debris from the electrical discharge. The addition of the blast ring provided the additional benefit of maintaining an increased path length to prevent surface arcing from electrode to electrode. An illustration of the insulator is shown in Fig. 4. The insulator was manufactured from an alumina ceramic with dimensions of 14.27 cm for the outer diameter, 9.04 cm for the inner diameter, and a thickness of 3.18 cm.

In a good number of HV switches elkonite is the electrode material of choice. For the anticipated Coulomb loading of this design it was felt that 70/30 elkonite, which is half tungsten and half copper by volume, would produce an excessive amount of copper deposition on the interior surfaces of the switch leading to earlier shorting of the electrodes. For this reason a material with a higher percentage of tungsten, HD18D, was selected to mitigate deposition of

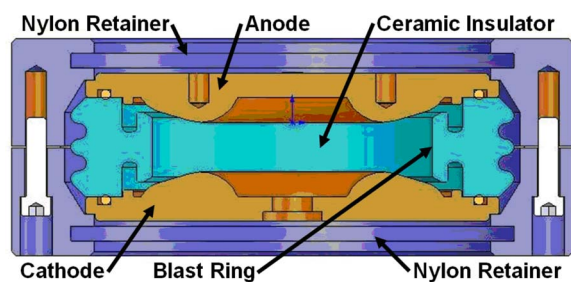


FIG. 3. (Color online) Assembly drawing.

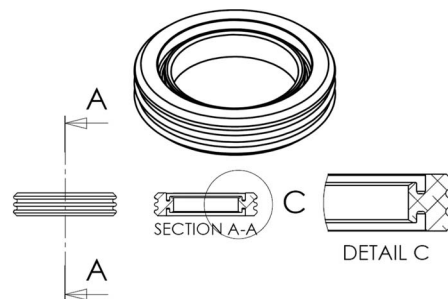


FIG. 4. Illustration of the insulator.

electrode material onto the insulating surfaces. This alloy is almost 95% tungsten. An illustration of this anode is shown in Fig. 5. Since HD18D is a metal powder which is pressed into a sheet, the authors found it prudent to coat the exterior surfaces with chrome to reduce the possibility of vacuum leakage due to microfractures. The anode has a diameter of 13.33 cm with a thickness of 1.59 cm. A lip was added just inside the o-ring groove to protect the o-ring from effects due to the discharge blast and to assist in centering the insulator on the electrode.

The trigger pins themselves consisted of standard Tele-dyne RISI RP-87 detonators without the explosives, the brass sleeve, or the stainless steel cup, refer to Fig. 6. The sleeveless detonators consisted of plastic cylindrical heads with two electrical wires extending axially through the plastic. As shown in Fig. 6 a bridge wire ran across one face of the plastic from electrical wire to electrical wire. Utilizing the detonator bridge wire as a fuse provided a charred surface on the face of the detonator, serving to condition the trigger pins, and hence increase their reliability. The spacing on the electrical pins of the detonators was of an appropriate dimension to produce a 5 kV spark with an energy of 0.25 J to initiate switch closure. Additionally, the insulation on the wiring of the pins provided sufficient electrical standoff to prevent inadvertent breakdown while awaiting a command

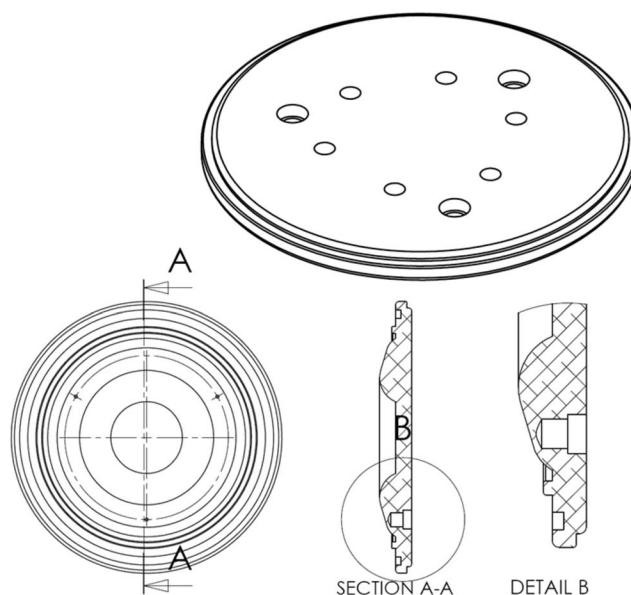
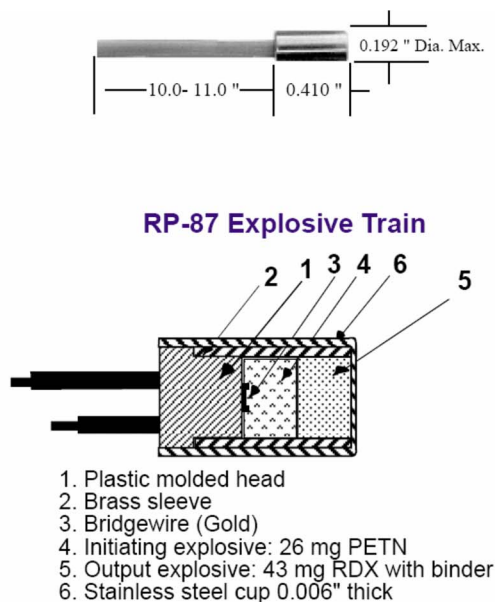


FIG. 5. Illustration of the anode.



#### RP-87 Firing Parameters

- Threshold Burst Current: 210 amps
- Threshold Voltage: Approx. 500 volts
- Threshold Voltage Std. Deviation: 75 volts maximum
- Function Time: 1.95  $\mu$ sec. typical
- Function Time Simultaneity Standard Deviation: 0.125  $\mu$ sec Max.

FIG. 6. (Color online) Illustration of the trigger pin.

fire signal. Note from Fig. 5 that the surface of the anode has been profiled to protect the three trigger pin ports from the effects of the discharge.

An illustration of the cathode is shown in Fig. 7. The cathode is a copy of the anode with the exceptions of the addition of a port for vacuum at the center of the electrode and the removal of the trigger pin ports.

### SWITCH PERFORMANCE

The performance of this design has been better than originally anticipated. The switch was originally envisioned as a switch which would carry approximately 100 kA and withstand 20 kV. COSMOS EMS studies, as shown in

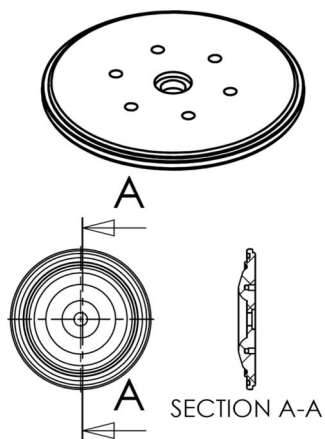


FIG. 7. Illustration of the cathode.

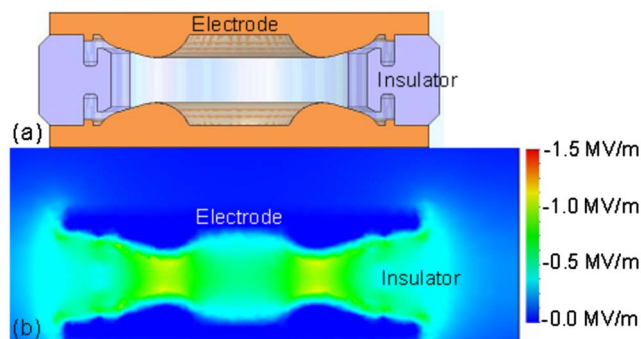


FIG. 8. (Color online) COSMOS EMS model of the switch interior.

Fig. 8, indicated that this design should be able to successfully withstand fields of this magnitude with all regions of electrical stress below approximately 1.2 MV/m. The current limitation of 100 kA was relaxed as the design gradually proved capable of carrying progressively higher and higher amounts of current.

While the design was required to hold off a maximum of 20 kV, it has been tested via a hi-pot tester to 30 kV, many times with no measurable current flow from anode to cathode. In those instances in which current flow was sensed, it was later found to be predominately traceable to either microleaks, typically about the trigger pins, or possibly to contaminated inner surfaces of the insulating ring. The microleaks produced localized areas of high pressure shifting the region of Paschen curve operation.

The electrodes were conditioned by subjecting the switch to a sequence of no less than ten 112 kJ pulses. Each pulse had an amplitude of approximately 95–100 kA, with a duration of approximately 0.5 ms. Switch vacuum and current parameters were monitored throughout the conditioning process to ensure the viability of the switch. Switches which did not condition properly were examined to determine the malfunctioning component(s) and were repaired and reconditioned when able.

Once successfully conditioned, each switch was installed in a PFN and was subjected to 1.2 MJ pulses. A plot of the current versus time for a typical switch installed in a PFN is shown in Fig. 9, with a plot of the action versus time shown in Fig. 10. Note in Fig. 9 that the maximum current carried by the switch was 308.9 kA. Higher current values were not attempted due to the limitations of the PFN utilized. Figure 10 shows the action achieved by the switch, which was 36.5 MA<sup>2</sup> s.

Self-break Paschen curve measurements were made of the switch. These are exhibited in Fig. 11. This illustrates that at the pressures at which the switch would typically operate ( $1 \times 10^{-6}$  Torr or less) and with an interelectrode gap of approximately 1.6 cm, the switch would typically be discharged in the field emission region of the Paschen curve.

The electrodes of a switch after 20 shots at 16 kV and 300 kA are shown in Fig. 12. Note the relatively uniform erosion pattern on the raised portions of the electrodes. The discharge pattern on both electrodes begins at approximately 3.6 cm in diameter and extends to approximately 6.6 cm in diameter, yielding an area of about 24.3 cm<sup>2</sup>. For a discharge



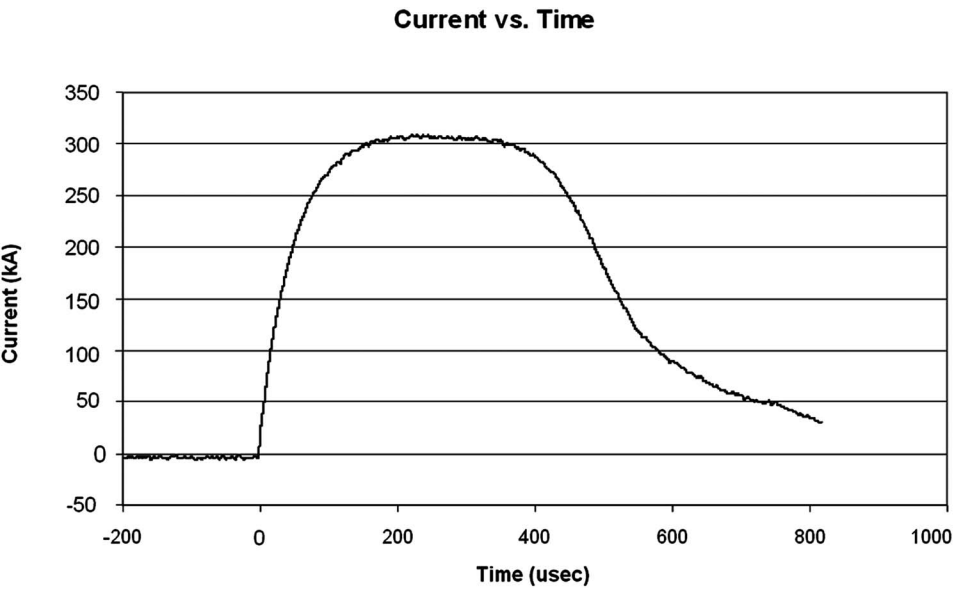


FIG. 9. Plot of current vs time for the vacuum switch.

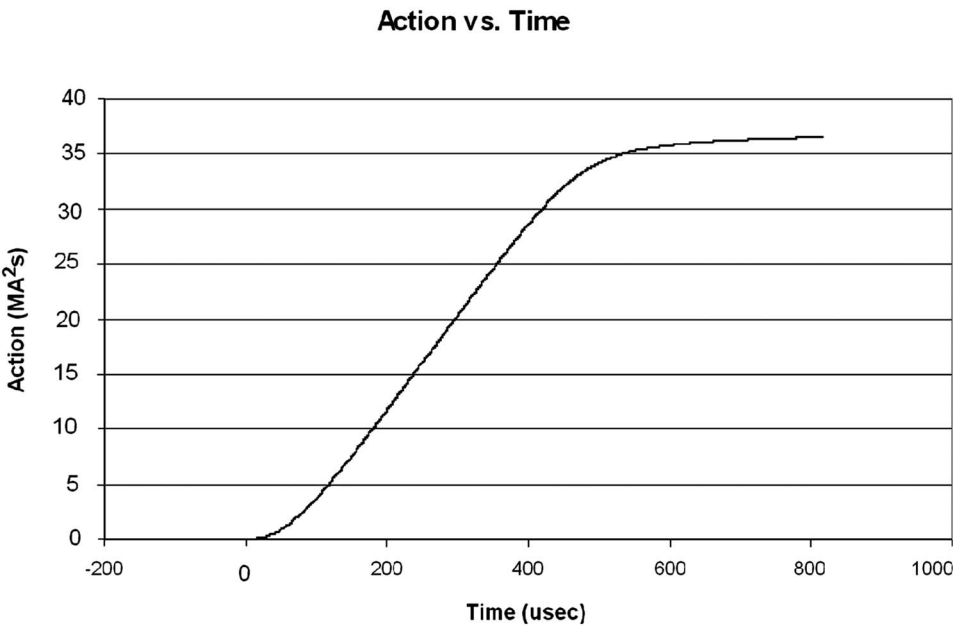


FIG. 10. Action vs time for the vacuum switch.

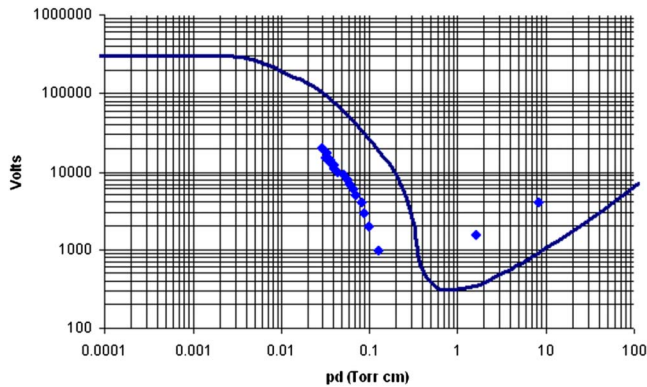


FIG. 11. (Color online) Paschen curve measurements of the switch.

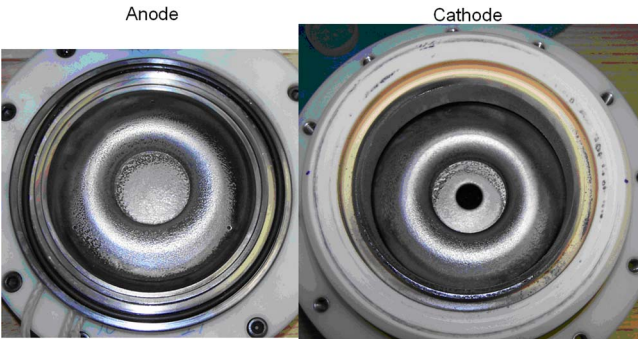


FIG. 12. (Color online) Electrodes after 20 shots at 16 kV and 300 kA.

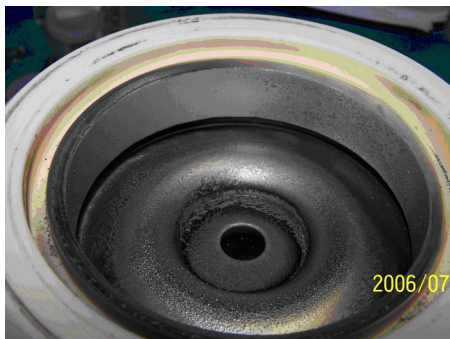


FIG. 13. (Color online) Insulator after 20 shots at 16 kV and 300 kA.

of 16 kV the Coulomb transfer across this area is approximately 150 C in 0.5 ms, yielding an average Coulomb transfer per area value of  $6.17 \text{ C/cm}^2$ .

Figure 13 shows the insulator from the same switch. Again note the relative cleanliness of the blast ring and the absence of deposition on the groove behind the blast ring. Some dust from the discharge can be seen residing in the groove, but the overall appearance of the groove demonstrates the utility of the blast ring in maintaining an extended surface track barrier.

Experiments performed with this switch have demonstrated the ability of this design to repeatedly switch 150 C within a period of 0.5 ms. The switch is capable of withstanding up to 20 kV, with testing being regularly done to 30 kV. Current flow has been measured at 308 kA, with the action calculated at approximately  $3.65 \times 10^7 \text{ A}^2 \text{ s}$ . Additional developments such as adjustments in the profile of the electrode face to produce a more uniform current distribution could yield compact switches capable of carrying 211 C.

## ACKNOWLEDGMENTS

The authors wish to acknowledge the invaluable contributions made to this work by Mr. Brian Costanzo, Mr. Brian Sobocinski, Mr. Rodney Reams, and Mr. Bruce Guffy.

- <sup>1</sup>I. M. Vitkovitsky, *High Power Switching* (Van Nostrand Reinhold, New York, 1987), p. 60.
- <sup>2</sup>H. Singh and C. R. Hummer, 12th IEEE International Pulsed Power Conference (IEEE, New Jersey, 1999), Vol. 2, pp. 1141–1144 and 27–30.
- <sup>3</sup>H. Singh and C. R. Hummer, *IEEE Trans. Magn.* **37**, 394 (2001).
- <sup>4</sup>A. Welleman, J. Waldmeyer, and E. Ramezani, *Proceedings of the LINAC 2002*, Gyeongju, Korea, 2002, pp. 709–711.
- <sup>5</sup>T. E. Podlesak, R. L. Thomas, Jr., and F. M. Simon, *IEEE Trans. Plasma Sci.* **33**, 1235 (2005).
- <sup>6</sup>S. Castagno, R. D. Curry, and E. Loree, *IEEE Trans. Plasma Sci.* **34**, 1692 (2005).
- <sup>7</sup>D. M. Giorgi, J. R. Long, D. M. Crosley, and T. Navapanich, 12th Symposium on Electromagnetic Launch Technology 2004, 2005, pp. 186–190 and 25–28.
- <sup>8</sup>D. F. Alferov, V. P. Ivanov, and V. A. Sidorov, 11th IEEE Pulsed Power Conference (IEEE, New Jersey, 1997), Vol. 2, pp. 857–861.
- <sup>9</sup>T. Warren, J. Dickens, A. Neuber, and M. Kristiansen, 12th IEEE International Pulsed Power Conference (IEEE, New Jersey, 1999), Vol. 2, pp. 1264–1267.
- <sup>10</sup>R. D. Ford, G. Dorr, R. Reams, and A. J. Toepfer, 11th IEEE Pulsed Power Conference (IEEE, New Jersey, 1997), Vol. 2, pp. 893–898.
- <sup>11</sup>R. Dethlefsen, V. A. Sidorov, and V. A. Vozdvijenskii, Eighth IEEE Pulsed Power Conference (IEEE, New Jersey, 1991), pp. 511–514.
- <sup>12</sup>Y. G. Chen, R. Dethlefsen, R. Crumley, V. A. Sidorov, and V. A. Vozdvijenskii, Ninth IEEE Pulsed Power Conference (IEEE, New Jersey, 1993), pp. 938–941.
- <sup>13</sup>M. E. Savage, 12th IEEE International Pulsed Power Conference (IEEE, New Jersey, 1999), Vol. 2, pp. 1264–1267.
- <sup>14</sup>S. S. Park, S. H. Nam, Y. J. Han, and B. Son, *IEEE Trans. Plasma Sci.* **33**, 192 (2005).
- <sup>15</sup>J. M. Lafferty, *Vacuum Arcs* (Wiley, New York, 1980), p. 328.

Review of Scientific Instruments is copyrighted by the American Institute of Physics (AIP). Redistribution of journal material is subject to the AIP online journal license and/or AIP copyright. For more information, see <http://ojps.aip.org/rsio/rsicr.jsp>